

On the Time Scale of Nocturnal Boundary Layer Cooling in Valleys and Basins and over Plains

STEPHAN F. J. DE WEKKER

National Center for Atmospheric Research, Boulder, Colorado*

C. DAVID WHITEMAN

University of Utah, Salt Lake City, Utah

(Manuscript received 12 July 2005, in final form 5 November 2005)

ABSTRACT

Sequences of vertical temperature soundings over flat plains and in a variety of valleys and basins of different sizes and shapes were used to determine cooling-time-scale characteristics in the nocturnal stable boundary layer under clear, undisturbed weather conditions. An exponential function predicts the cumulative boundary layer cooling well. The fitting parameter or time constant in the exponential function characterizes the cooling of the valley atmosphere and is equal to the time required for the cumulative cooling to attain 63.2% of its total nighttime value. The exponential fit finds time constants varying between 3 and 8 h. Calculated time constants are smallest in basins, are largest over plains, and are intermediate in valleys. Time constants were also calculated from air temperature measurements made at various heights on the sidewalls of a small basin. The variation with height of the time constant exhibited a characteristic parabolic shape in which the smallest time constants occurred near the basin floor and on the upper sidewalls of the basin where cooling was governed by cold-air drainage and radiative heat loss, respectively.

1. Introduction

The boundary layer warms during daytime and cools during nighttime in response to the changing available energy at the earth's surface. Around sunset when the available energy becomes negative, temperatures start to fall and a stable or nocturnal boundary layer forms. The boundary layer continues to cool during the night, leading to a surface temperature minimum near sunrise. Because good forecasts of minimum temperatures have an important practical value that extends to fog and frost predictions, a number of investigators have attempted to model the nocturnal cooling. A simplified analytical model developed by Brunt (1939) and later extended by Groen (1947) predicts the decrease in sur-

face temperature using a balance between net radiative loss at the surface and ground heat flux. Assuming that the net radiation and ground heat flux are constant during the night, the model predicts that surface temperatures will decrease with the square root of time. Using the same consideration of the heat balance at the surface but allowing the net radiation and ground heat flux to change with time, Whiteman et al. (2004b) derive an expression for the decrease of surface temperature in a basin that follows an exponential function. Pattantyús-Ábrahám and Jánosi (2004) show a good fit of screen-level temperature observations over flat plains with an exponential function. In contrast to the square root function, the exponential function allows the determination of a time constant that can be interpreted as a characteristic cooling time scale in the case of nocturnal cooling.

Although nocturnal cooling has been studied at the surface by the investigators mentioned above, nocturnal cooling through the entire depth of the boundary layer has received less consideration. This cooling is the result of a volumetric atmospheric heat balance rather than a balance of surface fluxes leading to a variation of

* The National Center for Atmospheric Research is sponsored by the National Science Foundation.

Corresponding author address: Dr. Stephan F. J. De Wekker, National Center for Atmospheric Research, P.O. Box 3000, Boulder, CO 80307-3000.
E-mail: dewekker@ucar.edu

temperature at the earth's surface (which is often equated to the temperature of the atmosphere at screen level just above the surface). Volumetric integrations are often preferred for comparison with atmospheric models, because they provide a more comprehensive evaluation of model physics and reduce the effects on the comparison of nonrepresentative surface sites. The major processes determining the rate of change of temperature in the boundary layer are advection and turbulent and radiative heat flux divergences. The importance of radiative flux divergence in the initial rapid cooling phase of the nocturnal boundary layer has been shown in various studies (e.g., André and Mahrt 1982; Sun et al. 2003).

Topography can affect the cooling in various ways. In valleys, cooling rates are affected by the presence of thermally driven slope and valley winds. Early in the evening, downslope flows develop along the sidewalls because radiative cooling at the sidewall surface and subsequent downward turbulent transfer of heat cause the layer of air adjacent to the slope to be colder than air at the same level away from the slope. The cold air flowing down the slopes converges over the valley floor, building up the inversion depth over time and resulting in inversions in valleys that are usually deeper than those over adjacent flat-terrain areas. The downslope flows that produce the convergence are usually accompanied by downvalley flows that carry the air cooled within the valley out the valley exit onto the adjacent plain. The cold air carried down the valley is replaced by potentially warmer air that subsides into the valley from aloft. This warm air decelerates the cooling, which, in turn, reduces the along-valley pressure gradient and the intensity of the valley wind system (Whiteman 2000). The complex interactions between advection and turbulent and radiative heat flux divergence make the theoretical prediction of nighttime cooling in the boundary layer very difficult. In perfectly closed basins, the complexity is reduced because horizontal advection is absent. Whiteman et al. (2004b) show that in these cases the total cooling on the basin floor may be primarily a function of the sky-view factor.

In the current paper, we use data to explore time-scale characteristics of boundary layer cooling in valley, basin, and plains atmospheres under undisturbed, clear-sky conditions. The variation with height of surface cooling in a basin is also investigated.

2. Approach

By integrating the potential temperature tendency $\partial\theta/\partial t$ over time t and height z from the surface to a given

height h we obtain the cumulative atmospheric heat storage per unit area (J m^{-2}):

$$H(t) = \int_0^h c_p \rho(t, z) \Delta\theta(t, z) dz, \quad (1)$$

where c_p is the specific heat of air at constant pressure, $\rho(t, z)$ is the air density, and $\Delta\theta(t, z) = \theta(t, z) - \theta(t_0)$ is the temperature difference between a given vertical profile of potential temperature at time t and a neutral potential temperature profile at an initial time t_0 . The height h corresponds to the height of the nocturnal inversion around sunrise when this layer is deepest.

To compare the accumulated cooling in valleys and basins of different size, we multiply the term within the integral of (1) by the factor $A(z)/A_h$, where $A(z)$ and A_h are the valley or basin drainage areas at heights z and h , respectively. This way, we obtain the "topography weighted" cumulative heat storage (J m^{-2}):

$$S(t) = \int_0^h c_p \rho(t, z) \Delta\theta(t, z) \frac{A(z)}{A_h} dz. \quad (2)$$

For the evaluation of $S(t)$ in a valley or basin we assume that $\Delta\theta(t, z)$ is horizontally invariant from sidewall to sidewall. Note that (2) can also be used for flat terrain if A is taken to be invariant with height.

In this paper, we calculate $H(t)$ for a variety of valleys and basins using sequences of tethersonde soundings over valley or basin centers from around sunset to around sunrise. A characteristic time scale for the nocturnal boundary layer cooling is then determined. The nocturnal inversion height h was determined subjectively from the plotted potential temperature profile of a near-sunrise sounding by selecting the level at which the strongly stable air in the valley or basin gave way to near-neutral background lapse rates above the stable layer. Continuity from sounding to sounding along with additional information from wind and humidity profiles was sometimes useful in determining this height. For the calculation of $S(t)$ in basins, $A(z)$ was determined from topographic maps and a planimeter. For valleys, $S(t)$ was determined for a unit-long valley segment from estimates of the valley floor width and the mean inclination angles of the two side slopes, and $A(z)$ is thus the valley width at a certain height times the 1-m length of the valley segment.

The initial time t_0 was taken as the latest time of day at which the potential temperature profile was approximately neutral. This time was usually about an hour before astronomical sunset. However, in snow-covered wintertime cases in which the inversion persisted during

the entire day and no neutral profile was observed, t_0 was taken as the time of the sounding nearest sunset. The final time in all cases was taken as the coldest sounding in the sequence, usually corresponding to a time near sunrise. To calculate $H(t)$ from individual soundings, temperature data were first interpolated to regular height intervals. In a few cases in which the near-sunrise sounding did not reach the inversion height, the soundings were extended by interpolation from previous and subsequent soundings.

3. Data

The data chosen for analysis were collected in high pressure weather with clear skies and weak upper-level winds, because these are the conditions that generally lead to the strongest inversions and cooling rates. The soundings were collected over the course of entire nights, but usually with the highest sounding frequency in the early evening to midevening. A near-sunrise sounding was required to meet the requirements of the experimental approach, and soundings had to be of sufficient depth to include the entire inversion layer. Data were available from a range of different valley, basin, and plains sites in different seasons, as shown in Table 1, which also lists the topographic characteristics of the sites. The accompanying Table 2 provides selected analysis results.

4. Results

a. Cooling of the stable boundary layer in valleys and basins and over plains

The cumulative cooling of the stable boundary layer was calculated from series of tethersonde ascents using (1) and (2). The cumulative cooling was then normalized by dividing $H(t)$ and $S(t)$ by the total accumulated nighttime cooling at (or near) sunrise, H_T and S_T , respectively. The H_T and S_T are calculated from (1) and (2) by setting $\Delta\theta(t, z) = \theta(t_{SR}, z) - \theta(t_0)$, where $\theta(t_{SR}, z)$ is the near-sunrise temperature sounding. The normalized total accumulated nighttime cooling values H/H_T (and S/S_T) were then plotted as a function of elapsed time $t - t_0$ (time since neutral profile) and were fit by two different functions, an exponential function

$$\frac{H}{H_T} = 1 - \exp\left(-\frac{t - t_0}{\tau}\right) \tag{3}$$

and a square root function

$$\frac{H}{H_T} = C(t - t_0)^{1/2}, \tag{4}$$

where τ is the fitting parameter for the exponential function and C is a constant. The fitting parameter characterizes the rate of cooling of the valley atmosphere, where τ is the time required for the cumulative

TABLE 1. Measurement sites, dates, and topographic characteristics.

Location	No.	Date	Lat	Lon	Valley depth (m)	Valley width (m)	Sidewall angles (°)	Drainage area (km ²)	Length of night (h)
Peter Sinks Basin, UT	1	8–9 Sep 1999	41.915°N	111.511°W	120	—	—	2.25	11.18
Gruenloch Basin, Austria	2	2–3 Jun 2002	47.821°N	15.045°E	120	—	—	1.82	8.23
Sinbad Basin, CO	3	15–16 Jul 1988	38.514°N	108.987°W	—	—	—	83.82	9.55
South Fork White River Valley, CO									
River Cabin	4	24–25 Aug 1978	39.974°N	107.625°W	300	*	*	448	10.6
River Cabin	5	28–29 Aug 1978	39.974°N	107.625°W	300	*	*	448	10.77
Mobley’s Y-Z Ranch	6	27–28 Aug 1978	39.955°N	107.584°W	350	400	18, 15	421	10.72
Mobley’s Y-Z Ranch	7	28–29 Aug 1978	39.955°N	107.584°W	350	400	18, 15	421	10.77
Yampa Valley, CO									
Sombrero Ranch	8	4–5 Feb 1978	40.458°N	106.814°W	450	2580	16, 09	1370	13.72
Sombrero Ranch	9	23–24 Feb 1978	40.458°N	106.814°W	450	2580	16, 09	1370	12.97
Horseshoeing School	10	9–10 Aug 1978	40.450°N	106.814°W	450	2580	16, 09	1370	10.05
Eagle Valley, CO									
Ray Miller’s Ranch	11	13–14 Oct 1977	39.641°N	106.571°W	700	1450	21, 10	1061	12.73
Gore Valley, CO									
Vail Safeway	12	9–10 Dec 1975	39.631°N	106.418°W	600	390	15, 16	233	14.92
Kansas Cooperative Atmosphere–Surface Exchange Study 1999 (CASES-99)	13	10–11 Oct 1999	37.65°N	96.73°W	—	—	—	—	12.55
Wangara, Australia	14–18	Jul 1967 (5)	34.5°S	144.93°E	—	—	—	—	13.9

* Valley width and sidewall angles could not be determined in this valley because of terrain complexity.

TABLE 2. Stable boundary layer characteristics.

Location	Integration (inversion) depth (m)	Inversion strength (°C) at sunrise	Max accumulated cooling (MJ m ⁻²)	Max accumulated cooling (topography weighted)	τ (h)
Peter Sinks Basin, UT	150	22	2.0	1.0	3.1
Gruenloch Basin, Austria	100	12	1.1	0.4	3.2
Sinbad Basin, CO	550	15	5.2	2.0	5.4
South Fork White River Valley, CO					
River Cabin	400	12	6.0	—	3.9
River Cabin	550	18	6.1	—	4.6
Mobley's Y-Z Ranch	550	14	8.1	3.7	5.5
Mobley's Y-Z Ranch	500	16	6.2	2.8	5.1
Yampa Valley, CO					
Sombrero Ranch	520	27	3.2	1.7	5.2
Sombrero Ranch	550	25	5.3	3.0	7.5
Horseshoeing School	600	17.5	6.0	3.0	4.4
Eagle Valley, CO					
Ray Miller's Ranch	510	15.5	9.7	5.4	6.4
Gore Valley, CO					
Vail Safeway	450	17	4.3	2.0	4.3
Kansas (CASES-99)	120	10	1.0	—	5.8
Wangara, Australia (five cases avg)	310	9.5	2.1	—	5.3

cooling to attain 63.2% [i.e., $(1 - e^{-1}) \times 100\%$] of its total nighttime value. The choice of the two functions was based on the theoretical considerations by Brunt (1939) and Whiteman et al. (2004b).

The results are shown for the basin, valley, and plains sites in Fig. 1. The square root fit overpredicts cooling rates at all locations in the first few hours of the night, whereas the exponential function provides suitable approximations to the data. The value of the reduced chi-square goodness-of-fit statistic was consistently smaller (indicating a better fit) for the exponential fit than for the square root fit. An error function fit (not shown) was similar to the exponential function fit.

Fits were obtained for all the sites and dates listed in Table 1. The computed time constant τ along with the integration depths, the inversion strengths at sunrise, and the maximum accumulated cooling calculated with and without topography weighting are provided in Table 2. Because normalization tends to make the H/H_T and S/S_T curves nearly coincident, we will discuss only the non-topography-weighted curves and calculations.

The basin atmospheres cool the fastest with $\tau = 3.1$ h, whereas typical values in flat terrain are around 5–6 h. The 3.9–5.5-h time constants for various locations inside the White River and Yampa Valleys on different days are intermediate between those of the small closed basins and the plains. Time constants can be much longer in snow-covered valleys when the previous night's inversion is still present at the beginning of the evening transition period. The normally high rates of

cooling associated with the evening transition period are greatly suppressed in this case. This result is shown for the snow-covered Yampa Valley (case 9), which had a time constant of 7.5 h. In the other two snow cases (cases 8 and 12), the previous night's inversion did not persist and time constants are comparable to the non-snow cases.

The results of the time-constant analysis for all of the locations and dates (Table 1) are shown in Fig. 2, where the time constant is plotted as a function of accumulated nighttime cooling. The total nighttime cooling varies greatly from site to site. The inversions that form in the small Peter Sinks and Gruenloch Basins (sites 1 and 2) are very shallow, as are the inversions that form over plains (13 and 14). Because their inversions are shallow, these sites experience small cumulative heat losses relative to the deeper valleys. A similarly broad range of time constants is also apparent among the sites, with the basins having the smallest time constants, the plains having the largest time constants, and the valleys having intermediate time constants. The Sinbad Basin is an apparent exception to the rule that basins will have short time constants, but Whiteman et al. (1996) have shown that the Sinbad Basin has a strong downvalley flow that occurs through a narrow drainage canyon and thus behaves more like a valley than a closed basin.

In general, as shown in Fig. 2, the time constants increase with the accumulated volumetric cooling. Thus, other conditions being equal, it takes longer to reach a certain amount of cooling in valleys that have a

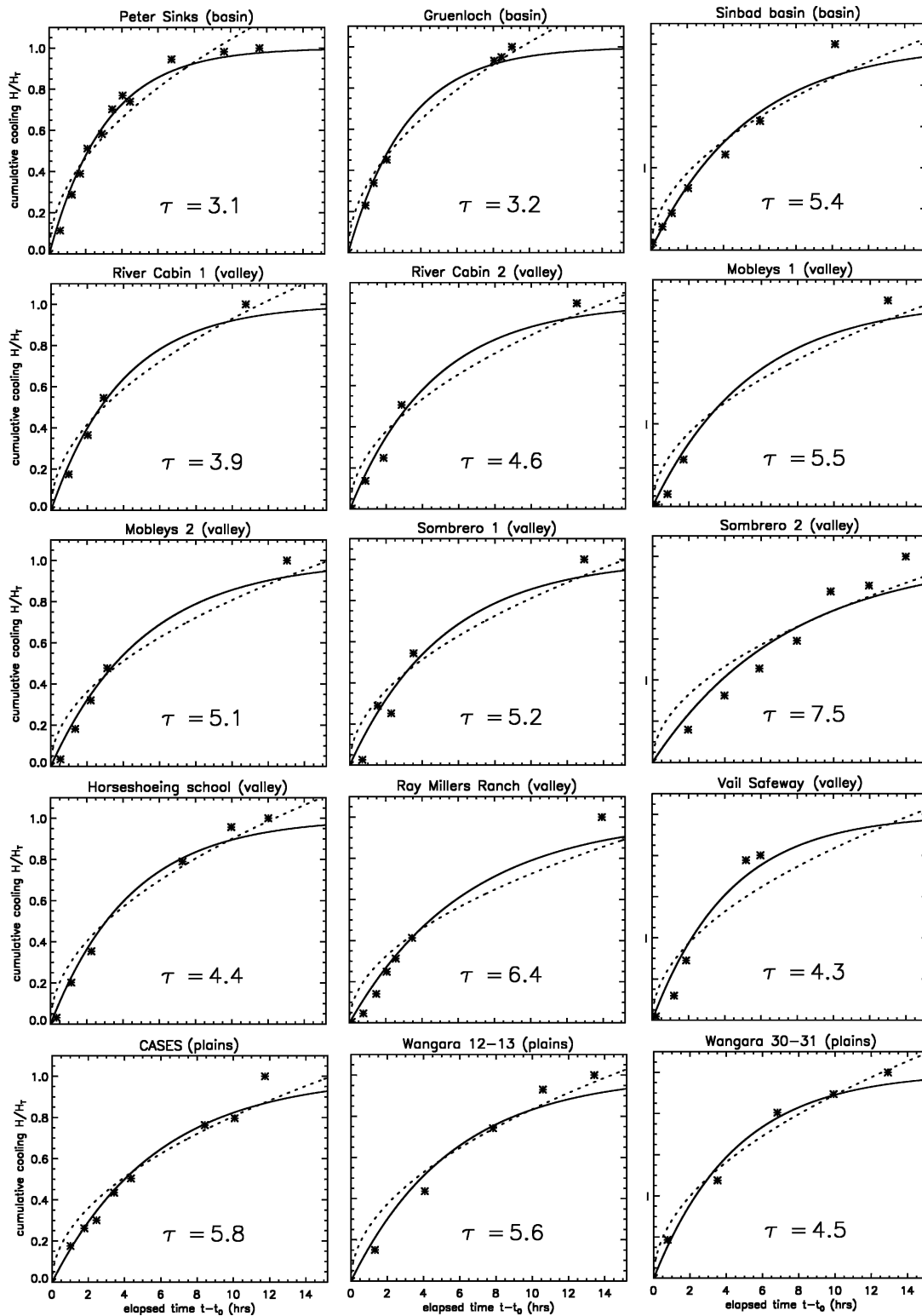


FIG. 1. Normalized cumulative cooling H/H_T as a function of elapsed time $t - t_0$ for the sites listed in Table 1. Solid and dashed lines are the exponential and square root fits to the data (asterisks); τ is the time constant for the exponential fit. Additional information on the terrain at each of the sites can be found in Table 1. Two of the five Wangara cases are shown in the figure.

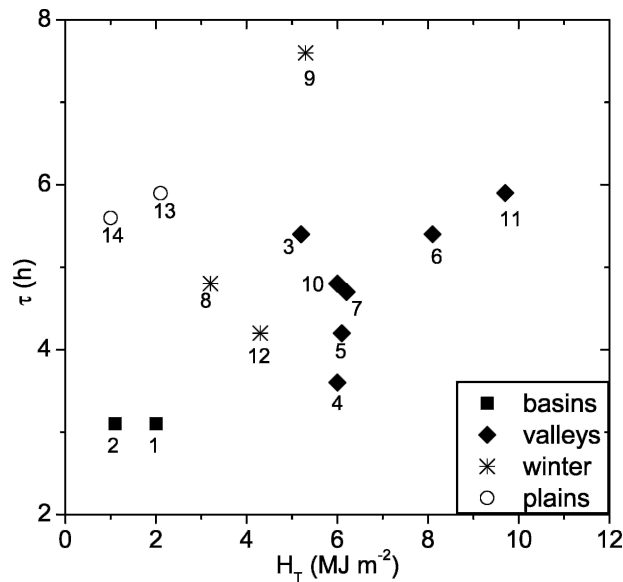


FIG. 2. Time constant (h) as a function of accumulated nighttime cooling for basins, valleys, and plains. The valley points include both snow-covered (asterisks) and non-snow-covered (solid diamonds) valleys. The numbers correspond to the station numbers in Table 1.

larger accumulated cooling. Of interest is that valleys with larger drainage areas do not necessarily possess larger accumulated cooling, implying that there is no clear relationship between time constant and drainage area. We do not have sufficient data from different seasons and a wide range of valley sizes to investigate this question further or to conclude whether an individual basin or valley location has a “typical” time constant, nor could we detect any clear dependency of the time constant on valley geometry or boundary layer characteristics such as inversion height and strength or average nighttime wind speed. Surface characteristics and ambient atmospheric conditions probably play important roles. An investigation of the factors that determine characteristic cooling time scales could be performed by numerical modeling. It is well known, however, that the simulation of nocturnal boundary layers is problematical and that numerical atmospheric models first need to be thoroughly evaluated before such an investigation can be made. The analysis of accumulated boundary layer cooling as presented in this paper could be a potential evaluation tool for such atmospheric numerical models. We plan to explore this application further.

b. Variation of cooling rates with altitude on basin sidewalls

In section 4a we calculated the cumulative cooling and time constants in atmospheric volumes enclosed in

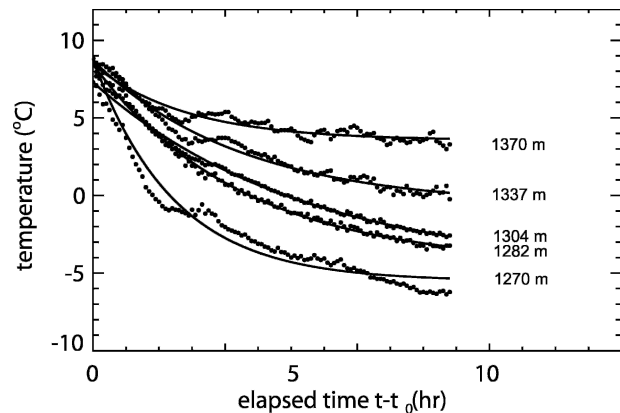


FIG. 3. Observed surface temperatures in the Gruenloch Basin on 2–3 Jun 2002 at five different elevations as a function of elapsed time $t - t_0$. The solid lines are best-fit exponential curves.

valleys or basins or in nocturnal stable boundary layers over plains. Earlier investigators (e.g., Pattantyús-Ábrahám and Jánosi 2004) computed cooling time constants for near-surface point temperature measurements over flat plains rather than for atmospheric volumes. To investigate the variation with height of time constants, we make time-constant calculations from two lines of surface-based temperature dataloggers exposed at 1.4 m AGL and running up the northwest and southeast sidewalls of the Gruenloch Basin (Whiteman et al. 2004a). Interpretation of the results requires knowledge of the topographic characteristics of the Gruenloch Basin. The basin is fully enclosed by topography from the basin floor (1270 m MSL) to the lowest saddle, or Lechner Saddle (1324 m MSL). Above this saddle, the basin is unconfined, and air cooled within the upper basin is known to flow out of the basin through the gap above this saddle. Typical inversion depths are about 120 m above the floor (1390 m MSL). Only the gap above the Lechner Saddle is an active air exit from the basin when inversions are 120 m deep. An example of the cooling curves and exponential function fits to the curves for five selected sites from the northwest line of dataloggers is shown in Fig. 3. The exponential function used to fit the data was

$$T(t) = (T_0 - T_c) \exp\left(-\frac{t - t_0}{\tau_{\text{exp}}}\right) + T_c, \quad (5)$$

where T_0 is the temperature at initial time t_0 [we use the same t_0 as in the calculation of $H(t)$] and T_c is the asymptotic cooling temperature. This function fits the observations well.

The approach illustrated in Fig. 3 was modified slightly to allow comparisons between the two lines of dataloggers in the Gruenloch Basin. Because of the effects of shadows and the exposure to the setting sun, the

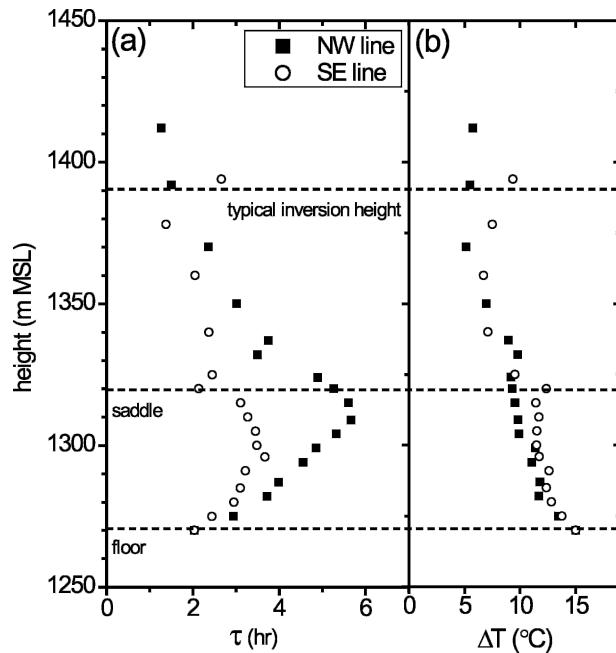


FIG. 4. (a) Time constant and (b) temperature drop from 1900 to 0405 CEST as a function of height for temperatures at 1.4 m AGL on lines running up the northwest and southeast sidewalls of Austria's Gruenloch Basin on 2–3 Jun 2002. The horizontal dashed lines denote the height of the basin floor, the lowest saddle (Lechner Saddle), and the typical temperature inversion top.

starting times for the evening transition cooling differed between the two sidewalls. To put the analyses on the same basis, we selected the time interval between 1900 and 0405 central European standard time (CEST) for the time-constant calculations. The 1900 CEST starting time was chosen because cooling was occurring on both sidewalls by this time, and the 0405 CEST ending time is the approximate time of sunrise. Astronomical sunset was at 1946 CEST.

The variation with height of the time constants τ and the drops in temperature ΔT during the selected time interval at the two lines of surface stations is depicted in Fig. 4. The temperature drop (Fig. 4b) is highest at the basin floor ($\sim 15^\circ\text{C}$) and decreases with height to attain about 5°C at and above the saddle. The drop during the time interval of interest is higher on the southeast sidewall than on the northwest sidewall, because the southeast sidewall is illuminated more directly by the setting sun. Whiteman et al. (2004a) show that the air temperatures in the Gruenloch Basin rapidly become equilibrated between the sidewalls after sunset when an inversion has started to form. The air enclosed in the basin below the saddle cools much more strongly than the air above the saddle because warmer air from aloft subsides into the upper basin as cold air drains through the gap above the saddle. These processes are the cause

of the sharp discontinuity in temperature drop at the altitude of the saddle on the southeast line and about 20 m above the saddle on the northwest line.

Time constants at the surface stations (Fig. 4a) vary parabolically with height and fall in a range from 1 to 6 h. They are shortest near the basin floor and in the upper basin near the inversion top. Note that this fact does not necessarily imply that the initial cooling rates are equally large near the basin floor and near the inversion top. Cooling rates depend not only on the time constant but also on the temperature drop during the night, as can be seen from differentiating (5) with respect to time:

$$\frac{dT(t)}{dt} = -\frac{1}{\tau_{\text{exp}}} (T_0 - T_c) \exp\left(-\frac{t - t_0}{\tau_{\text{exp}}}\right). \quad (6)$$

Therefore, because ΔT (which is proportional to $T_0 - T_c$) is smallest above the saddle, the absolute cooling rate is relatively small there in comparison with the cooling rate near the basin floor. The maximum time constants are found in the upper part of the enclosed basin just below the saddle where neither the radiative losses nor the accumulation of cold air by drainage are effective in producing local cooling. The shapes of the time-constant profiles are similar on the two sidewalls (i.e., parabolic), but time constants are smaller on the southeast line than on the northwest line. This situation would be consistent with larger longwave radiative losses from the warmer southeast sidewall. The shapes of the time-constant profiles were not sensitive to the choice of different starting times, and the basic features of the time-constant profiles were also observed for the following night of 3–4 June 2002.

Whiteman et al. (2004a) showed that the temperature measurements along the sidewall can be used as a proxy for vertical temperature profiles in the basin atmosphere at night. The time constants calculated this way averaged 2.8 h for the northwest and southeast lines. Remember from Table 2 that the time constant for the cooling of the basin atmospheric volume (calculated from tethered balloon measurements in the basin center) was 3.1 h for the Gruenloch Basin. This close agreement supports the conclusion by Whiteman et al. (2004a) that measurements on the sidewall and in the basin center are comparable at night.

5. Conclusions

The volumetric cumulative cooling in nighttime stable boundary layers that form in valleys and basins and over flat terrain on clear, undisturbed nights increases with time following an exponential shape rather than a square root shape. The square root fit overpre-

dicts cooling rates at all locations in the first few hours of the night. The cooling rates vary significantly among the individual valley, basin, and plains locations chosen for the analysis. An exponential fit to the observed accumulated cooling curves allowed us to calculate a volumetric time constant that can be interpreted as a nocturnal cooling time scale. The time constants are in the range from 3 to 8 h, indicating that 63.2% of the cumulative nocturnal cooling occurs over this time interval. The calculated time constants were shortest in small enclosed basins, were longest in nocturnal boundary layers that form over plains, and were intermediate in valleys. The time constants can be very long in snow-covered valleys, where inversions may persist for multiple days. We do not have enough data from multiple nights in the same valley or basin locations to determine whether a time constant might be a useful parameter describing cooling in individual valleys or basins.

An analysis of point temperature data from multiple locations on the sidewalls of the Gruenloch Basin revealed that the cooling time constants for point locations are altitude dependent and vary within a range from 1 to 6 h. The shortest time constants were found on the upper sidewalls of the basin and at the basin floor. The maximum time constant occurred below the saddle in the upper part of the fully enclosed lower basin. Preliminary hypotheses have been presented to relate variations in cooling rates to radiative transfer and air drainage effects.

In this paper, we have explored the use of a characteristic cooling time scale or time constant in the investigation of the nocturnal boundary layer in valleys and basins and over plains. It is clear that more data and research are needed to understand characteristic cooling time scales and their application fully. We argue that the analysis in terms of time constants presented here can be used as an evaluation tool for atmospheric numerical models. We plan to explore this application in a future paper.

Acknowledgments. Research support was provided by the U.S. Department of Energy's (DOE) Vertical Transport and Mixing (VTMX) program under the auspices of the Environmental Meteorology Program of the Office of Biological and Environmental Research. The research was conducted partly at Pacific Northwest National Laboratory, which is operated for DOE by Battelle Memorial Institute. SFJD acknowledges support from a postdoctoral fellowship from the Advanced Study Program at the National Center for Atmospheric Research. We thank Thomas Haiden and Jielun Sun for their comments on the manuscript.

REFERENCES

- André, J. C., and L. Mahrt, 1982: The nocturnal surface inversion and influence of clear-air radiative cooling. *J. Atmos. Sci.*, **39**, 864–878.
- Brunt, D., 1939: *Physical and Dynamical Meteorology*. 2d ed. Cambridge University Press, 428 pp.
- Groen, P., 1947: Note on the theory of nocturnal radiational cooling of the earth's surface. *J. Meteor.*, **4**, 63–66.
- Pattantyús-Ábrahám, M., and I. M. Jánosi, 2004: What determines the nocturnal cooling timescale at 2 m? *Geophys. Res. Lett.*, **31**, L05109, doi:10.1029/2003GL019137.
- Sun, J., S. P. Burns, A. C. Delany, S. P. Oncley, T. W. Horst, and D. H. Lenschow, 2003: Heat balance in the nocturnal boundary layer during CASES-99. *J. Appl. Meteor.*, **42**, 1649–1666.
- Whiteman, C. D., 2000: *Mountain Meteorology: Fundamentals and Applications*. Oxford University Press, 355 pp.
- , T. B. McKee, and J. C. Doran, 1996: Boundary layer evolution within a canyonland basin. Part I: Mass, heat, and moisture budgets from observations. *J. Appl. Meteor.*, **35**, 2145–2161.
- , S. Eisenbach, B. Pospichal, and R. Steinacker, 2004a: Comparison of vertical soundings and sidewall air temperature measurements in a small Alpine basin. *J. Appl. Meteor.*, **43**, 1635–1647.
- , T. Haiden, B. Pospichal, S. Eisenbach, and R. Steinacker, 2004b: Minimum temperatures, diurnal temperature ranges and temperature inversions in limestone sinkholes of different size and shape. *J. Appl. Meteor.*, **43**, 1224–1236.